Homopolymer and Block Copolymer Brushes on Gold by Living Anionic Surface-Initiated Polymerization in a Polar Solvent

GEORGIOS SAKELLARIOU,[1] MIKYOUNG PARK,[2] RIGOBERTO ADVINCULA,[2] JIMMY W. MAYS,[3,4] NIKOS HADJICHRISTIDIS[1]

[1]Department of Chemistry, University of Athens, 15771, Zografou, Athens, Greece

[2]Department of Chemistry, University of Houston, Houston, Texas 77204

[3]Department of Chemistry, University of Tennessee, Knoxville, Tennessee 37996

[4]Oak Ridge National Laboratory, Oak Ridge, Tennessee 37830

Received 11 October 2005; accepted 11 October 2005
DOI: 10.1002/pola.21195
Published online in Wiley InterScience (www.interscience.wiley.com).

ABSTRACT: Living anionic surface-initiated polymerization on flat gold substrates has been conducted to create uniform homopolymer and diblock copolymer brushes. A 1,1-diphenylethylene (DPE) self-assembled monolayer was used as the immobilized precursor initiator. *n*-BuLi was used to activate the DPE in tetrahydrofuran at –78 °C to initiate the polymerization of different monomers (styrene, isoprene, ethylene oxide, and methyl methacrylate). Poly(styrene) (PS) and poly(ethylene oxide) (PEO) in particular were first investigated as grafted homopolymers, followed by their copolymers, including poly(isoprene)-*b*-poly(methylmethacrylate) (PI-*b*-PMMA). A combined approach of spectroscopic (Fourier transform infrared spectroscopy, surface plasmon spectroscopy, ellipsometry, X-ray photoelectron spectroscopy) and microscopic (atomic force microscopy) surface analysis was used to investigate the formation of the polymer brushes in polar solvent media. The chemical nature of the outermost layer of these brushes was studied by water contact angle measurements. The effect of the experimental conditions (solvent, temperature, initiator concentration) on the surface properties of the polymer brushes was also investigated. © 2005 Wiley Periodicals, Inc. J Polym Sci Part A: Polym Chem 44: 769–782, 2006

Keywords: anionic polymerization; surface polymerization; self-assembled monolayer; polymer brushes; FTIR; AFM

INTRODUCTION

Polymer brushes on solid substrates are attracting increasing attention because of their ability to tailor the surface properties of these inorganic materials.[1–3] In particular, diblock copolymer brushes evoke great interest because of their potential applications in a variety of technological fields from adhesion to biomedical applications.[4–7] Moreover, it is important to develop understanding of how the immobilized chain end along with the interaction parameter, χ, and the surface energy, γ, of each block affects the tendency for microphase separation of the diblock copolymer brushes.

Correspondence to: N. Hadjichristidis (E-mail: hadjichristidis@chem.uoa.gr); R. Advincula (E-mail: radvincula@uh.edu)

Journal of Polymer Science: Part A: Polymer Chemistry, Vol. 44, 769–782 (2006)
©2005 Wiley Periodicals, Inc.

The fabrication of tethered polymers can be achieved by two different approaches. The first approach involves physical adsorption or physisorption. This case can occur, either by the use of end-functionalized polymers with zwitterionic end-groups[8] or by the selective physical adsorption of diblock copolymers,[9] where a shorter "anchor" block adsorbs strongly onto the surface leaving the remaining "buoy" block tethered to the interface. However, this method has the disadvantage of solvolytic and thermal instability due to the low interaction between the polymer and the substrate. The second approach involves the covalent attachment or chemical adsorption (chemisorption) of the polymer chains onto the surface. The two possible ways to accomplish the covalent attachment are the so-called "grafting-onto"[10] and "grafting-from" techniques. Regarding the grafting-onto technique, end-functionalized polymers are synthesized and covalently reacted with the appropriate substrates. Both physisorption and grafting-onto are self-limiting techniques with regards to the polymer film thickness and the grafting density. Every adsorbed polymer molecule "wants" to maintain the random coil conformation it adopts in solution. Therefore, the additional polymer chains have to diffuse through the already adsorbed layer to react with the available grafting sites. Consequently, the concentration of the polymer chains close to the interface becomes much higher than the solution and the diffusion becomes sterically and kinetically hindered. To circumvent these limitations, another promising technique, "grafting-from,"[11–48] is used. The grafting-from technique is accomplished using surface immobilized initiators. Hence, small molecules (the monomers), rather than big polymer chains, have to diffuse to react with the initiation sites, and the polymerization is promoted in the direction normal to the substrate. The immobilized initiators can be obtained, either by treating the substrate with plasma or glow-discharge[49–52] or by the self-assembled monolayer (SAM) technique.[53] The utilization of SAMs as the initiator sites for surface-initiated polymerization provides the opportunity to prepare well-defined, highly dense, polymer brushes.

Polymer brushes resulting from the grafting-from technique have been synthesized from flat substrates,[11–28] silica and gold nanoparticles[29–45] and carbon nanotubes,[46–48] via a number of polymerization mechanisms, including free-radical, cationic, anionic, atom transfer radical (ATRP), ring opening metathesis polymerization (ROMP), reversible addition-fragmentation transfer (RAFT), and nitroxide-mediated radical polymerization (NMRP).

To obtain a uniform, well-defined diblock copolymer brush, the polymerization mechanism must fulfill certain criteria. First, the mechanism must be living. This means that block copolymers can be obtained by sequential addition of monomers. The tethered polymer chains must also grow simultaneously from the well-packed (high grafting density) initiator sites of the SAM to obtain brushes with low polydispersity indices and good control of the molecular weight. Anionic polymerization is known to provide the best control over molecular weight and molecular weight distribution, leading to the synthesis of well-defined block copolymers. In addition, the synthesis of more complex macromolecular architectures can be achieved through this polymerization method.[54–55]

We have previously reported the living anionic surface-initiated polymerization of styrene and diene homopolymers as well as diblock copolymer brushes on silicon and gold wafers in benzene. 1,1-Diphenylethylene (DPE) with chlorosilane and thiol end-groups, tethered by the self-assembled technique, was the initiator precursor.[21,37] The Quirk group has likewise reported the tethering of homopolymers and copolymers using DPE on a variety of substrate surfaces.[23]

In this paper, we report the synthesis and characterization of homopolymer and block copolymer brushes on gold substrates in a polar solvent (tetrahydrofuran, THF) with a variety of monomers (styrene (St), isoprene (I), ethylene oxide (EO), and methyl methacrylate (MMA)). We first focused on poly(styrene) (PS) and poly(ethylene oxide) (PEO) homopolymers. In particular, the grafting of PEO or polyethylene glycol (PEG) is of high interest because of their protein resistant properties and interesting interaction with water molecule structures.[31] Eventually, the goal was to synthesize thick, uniform polymer brushes with high grafting density, using a polar solvent, which is deemed to be more favorable for surface-initiated living anionic polymerization. The generality to block copolymer synthesis was applied towards poly(isoprene)-*b*-poly(methylmethacrylate) (PI-*b*-PMMA) brush formation. The effect of monomers with different surface energies on the observed morphology of diblock copolymer brushes will also be discussed.

EXPERIMENTAL

Materials

Solvents [benzene (Aldrich, >99%), THF (Aldrich, 99.9%), hexanes (Aldrich, 99.9%)], monomers [styrene (Aldrich, 99%), isoprene (Aldrich, 99%), ethylene oxide (Aldrich, 98%), methyl methacrylate (Aldrich, 99%)], and terminating reagent (methanol) were purified according to standard procedures.[56] Phosphazene base (P_4, Aldrich, 1.0 M in hexanes) was used as additive to facilitate the anionic polymerization of ethylene oxide, using an organolithium anionic initiator. It was dried under vacuum for at least 12 h and diluted by distilling purified THF through the high vacuum line. The solution was sealed in a glass apparatus equipped with break-seals. *n*-Butyllithium was synthesized by the reaction of *n*-butyl chloride (Aldrich, 98%) and lithium metal (Aldrich, 99.99%) and was used as the polymerization initiator.

Characterization Techniques

X-ray spectroscopy (XPS) was carried out with a Kratos Axis 165 Multitechnique Electron Spectrometer system. A monochromatic Al Kα X-ray source (1486.6 eV) operated at 15kV and 20 mA was employed to excite the photoelectron emission at $\theta = 0$ (normal to the surface). Fixed analyzer transmission (FAT) mode was used, and survey scans (spot of 800 $\times$ 200 μm^2 resolution 4 eV at analyzer pass energy of 160 V) were collected from 0 to 1400 eV to obtain elemental composition of the polymer film. The C1s peak of hydrocarbon signal (284.5 eV) was used as the binding energy reference. The charge build-up during the measurements was compensated by a built-in charge neutralizer.

The surface plasmon spectra (SPS) were measured using the SPS mode of the Multiskop with a Kretschmann configuration and attenuated total reflection conditions.[57] The reflectance was monitored with a p-polarized He–Ne laser ($\lambda = 632.8$ nm) as a function of the angle of incidence.

The polymer film morphologies were studied by atomic force microscopy (AFM) using a PicoScan system (Molecular Imaging) equipped with an 8 $\times$ 8 micro scanner. A magnetic AC (MAC®) mode was used for all AFM images. MAC lever®, a silicon nitride-based cantilever coated with magnetic film, was used as the AFM tip. The force constant of the tip was 0.5 N/m with a resonance frequency of approximately 100 kHz. All samples were measured inside a suspension chamber to minimize ambient disturbance.

Infrared (IR) spectra were obtained using a Nicolet NEXUS 470 FTIR system, with a grazing incidence angle attachment for specular or low angle measurements on Au-coated glass substrates ($\sim$450 Å). Polarization modulation infrared reflection absorption spectroscopy (PM-IRRAS) measurements were also made with the gold-coated glass substrates. The spectra were obtained using a Nicolet MAGNA-IR 860 spectrometer equipped with a liquid nitrogen-cooled mercury–cadmium–teluride (MCT) detector and a Hinds Instruments PEM-90 photoelastic modulator (37 kHz). The light was reflected from the samples at an 80° angle and collected over 256 scans at a spectral resolution of 4 cm^{-1}.

^1H and ^{13}C NMR experiments were performed on a Bruker ARX-300 spectrometer (Bruker Instruments, Karlsruhe, Germany). Typical parameter settings include temperature = 305 K, relaxation delay = 4 s, solvent = $CDCl_3$. The internal standard was the residual proton chloroform signal of deuterated chloroform (7.24 ppm downfield from tetramethylsilane).

The advancing and receding water (Milli-Q) contact angles were measured using the sessile drop technique—contact angle goniometer (MicroCAM, Tantec).

A Quartz Crystal Microbalance (QCM; Maxtek Inc.), with a phase-locked PLO-10 oscillator and PM-740 frequency counter, was used to measure the mass and density of the DPE initiator. The quartz crystal electrode was modified by SAM formation of the thiol initiator.

Ellipsometric thickness measurements were performed using the Multiskop ellipsometer (Optrel GmbH, Germany), with a 632.8 nm He–Ne laser beam as the light source at 70° angle of incidence. Both delta and psi values (thickness data) were measured and calculated using integrated specialized software that was provided with the instrument.

Immobilization of the Initiator Precursor

The SAM of the DPE initiator was prepared as follows: the gold-coated glass substrates were treated with plasma cleaning (under Ar, using PLASMOD, March Instruments). The substrates were thoroughly rinsed with Milli-Q purified water and dried in an oven (90 °C) overnight before use. Modified gold-coated quartz crystals (QCM substrates) were plasma-treated under O_2 followed by

Ar conditions. The procedure for the thiol-DPE SAM formation on Au involved dipping the substrate into the dry toluene solutions of the initiator (10^{-4} M in toluene for 3 h) and subsequent copious washing with toluene. All the surfaces were characterized before and after polymerization.

Polymerization Procedure for the PS Homopolymer Brush

The all-glass apparatus used in the synthesis is shown in Figure 1. After placing the SAM-coated substrate (with DPE moiety) in the reactor, the glass apparatus was docked to the high vacuum line. A volume of 50 mL of purified THF was distilled from a reservoir containing liquid K/Na alloy (3:1 by weight) through the high vacuum line to the purge section. This reactor was flame-sealed from the high vacuum line (A). The purge section was placed in a dry ice–isopropanol bath at −78 °C and then *n*-BuLi (7 mL, 1 M in hexane) and 0.5 mL of neat DPE were introduced into the purge section by rupturing the corresponding break-seals. This solution was used to clean the inner walls of the reactor. Then this solution was kept at −78 °C for 1.5 h and a portion of the excess *n*-BuLi reacted with the DPE moiety on the substrate. The solution was transferred into the purge section and clean solvent was back distilled into the reactor. By doing this, all impurities and excess *n*-BuLi were collected in the purge section, which was subsequently removed by flame-sealing the constriction (B). Styrene monomer (10 g) was distilled into the reactor. The polymerization of styrene was allowed to proceed for approximately 12 h at −78 °C before terminating with 2 mL of degassed methanol.

Polymerization Procedure for the PEO Homopolymer Brush

The preparation of the initiator-bound substrate and the cleaning of the reactor are the same as described above. The ethylene oxide monomer (10 g) was added to the reactor by rupturing the corresponding break-seal. The reactor was kept at room temperature for 1 h before the addition of the phosphazene base *t*-BuP_4 (10^{-3} mol). The polymerization was allowed to proceed for 8 days at 40 °C.

Polymerization Procedure for the PS-*b*-PEO Block Copolymer Brush (Scheme 2)

The procedure adopted for the polymerization of the PS block was similar to the one described here for the homopolymer brush. The polymerization of the styrene (10 g) was allowed to proceed for 4 h at −78 °C, followed by addition of the second monomer ethylene oxide (5 g) into the reactor. The temperature was gradually increased to room temperature, and after one hour phosphazene base *t*-BuP_4 was introduced into the reactor. The polymerization of the second monomer was allowed to proceed for 8 days at 40 °C.

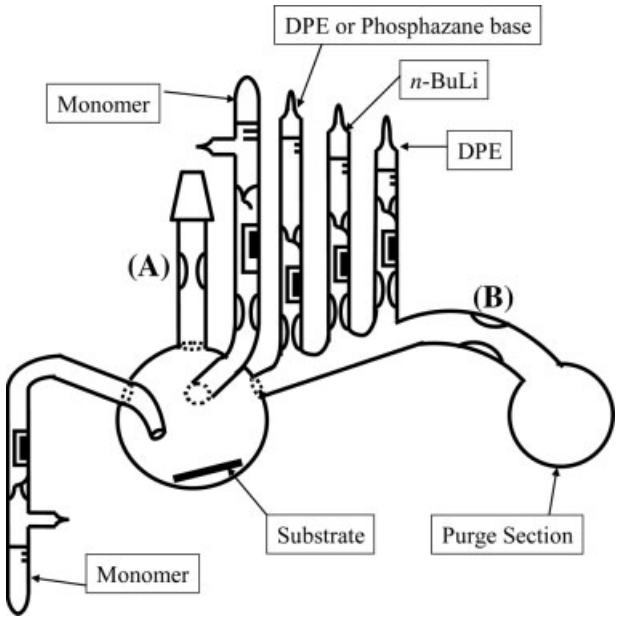

Figure 1. Polymerization reactor for the synthesis of homopolymer and block copolymer brushes.

Polymerization Procedure for the PI-*b*-PMMA Block Copolymer Brush (Scheme 3)

The polymerization of isoprene was conducted following the same procedure as that for the polymerization of styrene. The polymerization of isoprene (10 g) was allowed to proceed for 4 h at −78 °C, followed by addition of 2 mL of DPE into the reactor. One hour later methyl methacrylate (5 g) was distilled into the reactor and was polymerized for another 3 h at −78 °C.

RESULTS AND DISCUSSION

SAM Formation

The detailed synthesis of the precursor initiator thiol-DPE (Scheme 1) and the complete characterization of the SAM-DPE by a number of sur-

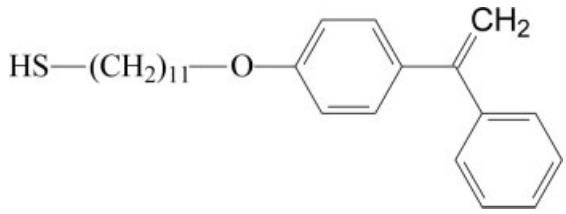

Scheme 1. The precursor initiator for the synthesis of self-assembled monolayers.

face-sensitive analytical techniques (ellipsometry, SPS, AFM, QCM, and contact angle) was reported in our previous work.[21] The formation of a uniform, well-packed, and characterized SAM on the substrate is very crucial for the whole procedure. Hence, by using thiol-DPE on gold surfaces, the SAM formation is facilitated by the absence of a native oxide layer on the substrate (not common for many metals), since the presence of such a layer can affect the polymerization mechanism. The precursor initiator thiol-DPE has a number of advantages. DPE is stable at high temperatures, and in various solvents, can react quantitatively with alkyllithium initiators and can polymerize styrenic, dienic, and (meth)acrylic monomers. It is also suitable because, due to steric reasons, it prevents the self-polymerization after activation with alkyllithium initiators parallel to the surface. In addition, the long alkyl spacer between the DPE and the thiol group is responsible for the formation of a well-packed monolayer, which provides high surface coverage. Finally, the precursor initiator can form a stable Au–S chemical bond on the substrate with respect to the temperature.

To prepare a polymer brush with high grafting density it is important to create as many initiation sites on the SAM as possible. For this reason, a number of polymerizations took place in custom-made glass reactors (Fig. 1) to estimate the appropriate reaction time for a large excess of *n*-BuLi to activate the DPE end-group of the SAM. Five Au substrates, having the same adsorbed amount of SAM-DPE as that estimated by QCM, were placed in five reactors and allowed to react with the same amount of *n*-BuLi for 0.5, 1, 1.5, 2.5, and 4 h at -78 °C. After the complete removal of the excess of *n*-BuLi, an equal amount of styrene was added in each reactor and all the polymerizations were allowed to proceed for 3 h before terminating with methanol. All substrates were washed many times with toluene. QCM measurements (monitoring frequency shift) indicated that there were no weight change in substrates after 1.5 h. Hence, 1.5 h is the estimated minimum time for the *n*-BuLi to create the maximum concentration of initiation sites on the Au surface.

Synthesis and Characterization of Tethered Homopolymer Brushes on Au Surfaces

Homopolymer brushes of PS and PEO were synthesized by means of anionic polymerization high vacuum techniques. The polymerizations were carried out in custom-made glass reactors (Fig. 1). In both cases, *n*-BuLi was used to activate the SAM-DPE on the surface. It was found that in THF at -78 °C, 1.5 h was adequate for a large excess of *n*-BuLi to react quantitatively with the DPE. It is important that the excess of the alkyllithium be removed before the addition of the monomer to ensure that the polymerization will propagate only from the surface and not in the solution. A number of research groups have reported the polymerization from both surface-immobilized initiators and free initiators in the solution, assuming that the propagation rate for both polymerizations was the same. We tried to avoid the polymerization in the solution because it would compete with the surface-initiated polymerization and may be much faster.

The polymerization of styrene was allowed to take place for 12 h at -78 °C before terminating with an ampoule of degassed methanol. Subsequently, the substrates were washed many times with toluene (until no change of the thickness was observed by SPS) to remove any possible adsorbed amount of polymer that had been polymerized in the solution. Thickness measurements were performed using SPS (Fig. 2), which identified a uniform PS film with an average thickness of 14 ± 0.2 nm. SPS is a highly sensitive technique for the characterization of ultrathin films. By monitoring angular-reflectivity changes before and after polymerization, we can obtain information on film formation and optical properties. The resonance angle and shape of the SPS curves are correlated to film thickness and dielectric constants, i.e., the refractive index. The thickness of these films was calculated based on the Fresnel algorithm fit of the SPS curves. The refractive index used was $n = 1.51$, which is typical value for these polymers.[58] The shape and position of the curves are functions of the thickness, d, and the refractive index, n. The film thickness was less than the values previously reported. The main difference between these works was the

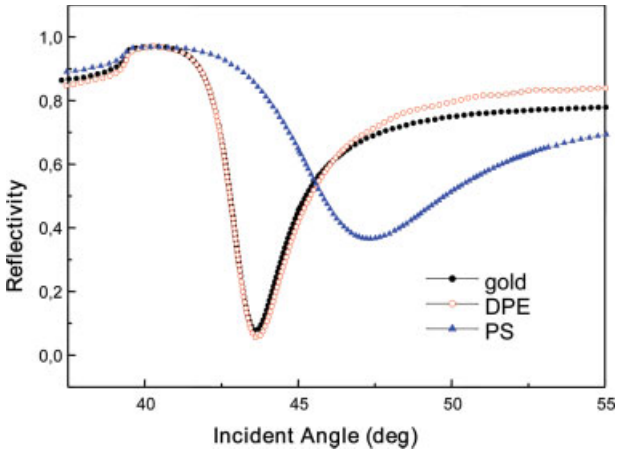

Figure 2. SPS spectrum of the PS homopolymer brush.

experimental conditions (solvent, THF) employed. Assuming that 12 h at −78 °C was sufficient for the polymerization of styrene in THF, we can conclude that the failure to obtain a thicker brush must be due to the solvent. THF is much more difficult to purify than benzene. Therefore, termination reactions are more likely to take place in this solvent, even at low temperatures. Considering that the polymerization propagates only from the surface and that the concentration of the initiation sites is extremely low, the impurities and termination reactions induce a crucial impact on the growth of the tethered polymer chains.

The wetting properties of the PS brush were measured by the advancing and receding water contact angles, using the sessile drop technique. Contact angles are very sensitive to the uppermost surface composition changes (sensing depth 0.5–1 nm), and many factors such as surface energy, roughness, and chemical heterogeneity can influence the estimated values. The advancing water contact was 94° ± 2° and the receding was 87° ± 2°, which are both very close to the bulk polystyrene reported values.

The XPS spectrum showed the carbon C 1s peak at 284.5 eV, together with a small "shake up" peak at 291 eV for the π-electrons (π to π^* transition), indicating the presence of PS on the surface (Fig. 3). The ratio of the C 1s peak is much higher with respect to the Au 4p and 4f peaks, further confirming the formation of a relatively thick PS brush with a high surface coverage.

To clarify the conformation of the PS brushes on the Au substrate, atomic force microscopy (AFM) was performed [Fig. 4(a)]. The surface topography was similar to that observed for the PS films on Au surfaces, using different polymerization conditions (solvent, temperature, initiator).[21] The film consists of smooth, uniform areas with a root-mean-square (RMS) roughness of 0.7 nm and defects (dimples) with a depth of 11–14 nm, corresponding to the film thickness. In contrast, the morphology that was observed on SiO_x substrates was influenced by the polymerization conditions (addition of polar solvent, amount of initiator used). Parameters such as grafting density, glass transition temperature, T_g, molecular weight, M_w, and polydispersity index of tethered polymer chains will greatly affect the conformation of the brushes on the substrate and thus the observed morphology. Comparing the AFM images of Au and SiO_x substrates, only the grafting density led to a different morphology. The SiO_x substrates have a consistent morphology made up of holes, surrounded by reliefs statistically distributed within the domains.[21] On the other hand, on the Au substrates the holes are much smaller and the relief structures more prominent. The possible reason for the low grafting density on SiO_x substrates is the attack of alkyllithium initiators in the presence of the polar additive (THF) to the Si—O—Si bonds and the removal of the surface-tethered initiator,[59] rendering these substrates unsuitable for such polymerization conditions.

The homopolymer PEO brush was synthesized using the same experimental procedure as that for PS. After activation of the SAM-DPE with the *n*-BuLi and the removal of its excess, the temperature was increased from –78 °C to room temperature and EO was added into the reactor by rupturing the break seal. After 1 h, 10^{-3} mol of phosphazene base (*t*-BuP_4) was added and the

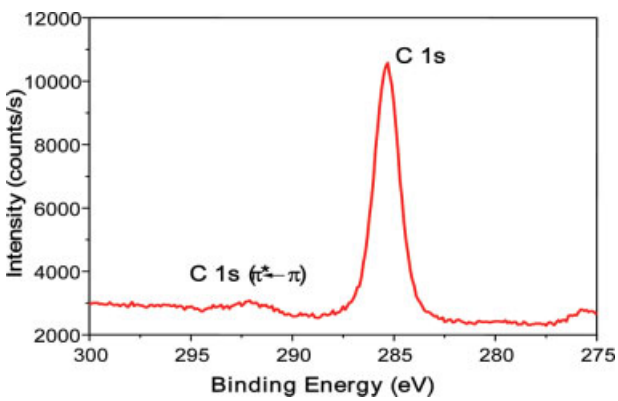

Figure 3. XPS spectrum of the PS homopolymer brush.

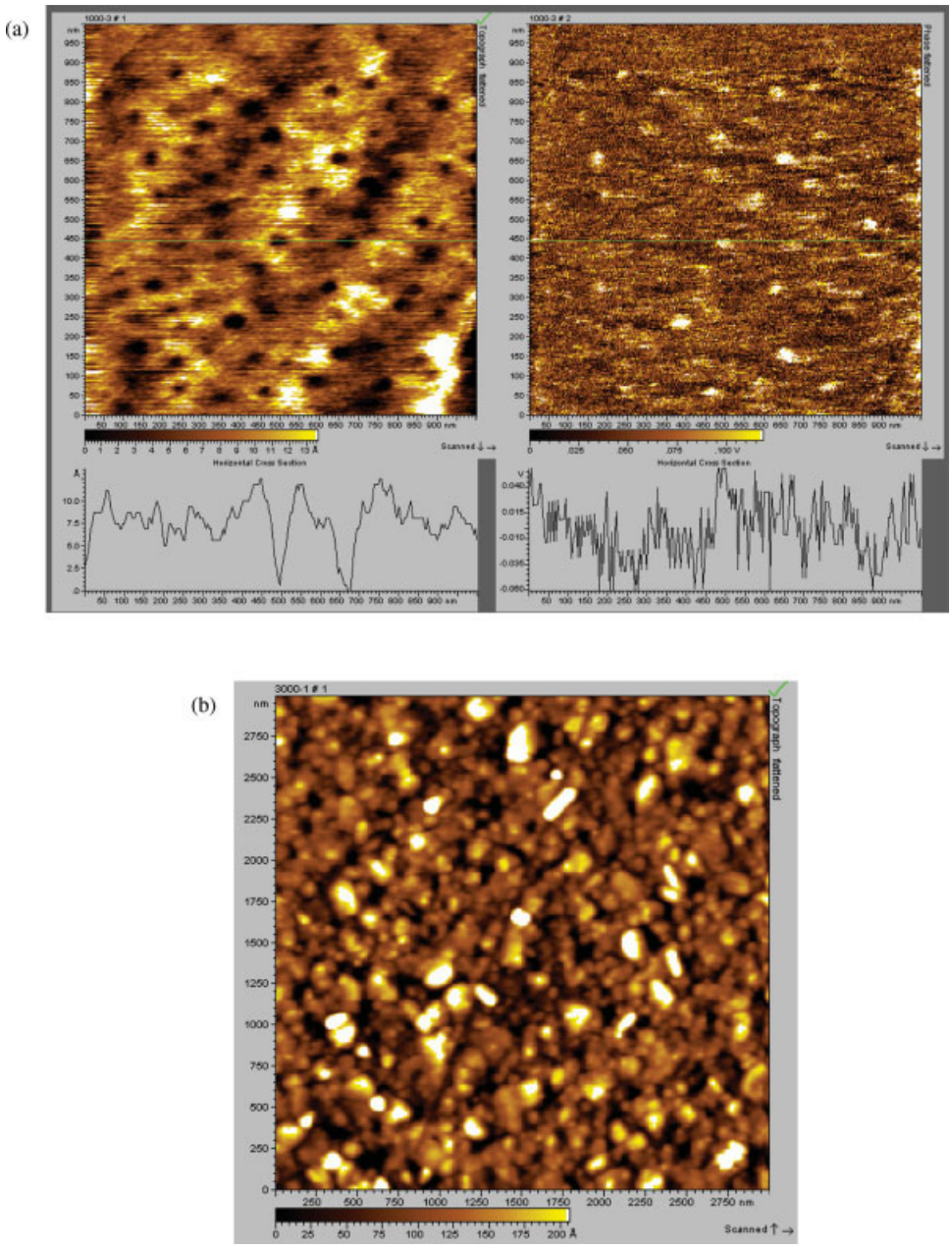

Figure 4. (a) AFM images of PS brushes. Topological or height image (left) and amplitude or phase image (right). (b) AFM images of PEO brushes. The topological or height image before annealing (left) and after annealing at 100 °C (right).

reaction temperature was increased to 40 °C. It is important that the temperature remains below 80 °C, because the Au–S bond is not stable above this temperature. The polymerization was allowed to proceed for 8 days at 40 °C before terminating with methanol.

SPS measurements indicated a 6-nm thin PEO polymer brush on the gold surface (Fig. 5). The XPS spectrum (Fig. 6) showed the relevant C 1s peak at 284 eV and the O 1s peak at 532 eV, indicating the presence of the PEO brush. However, relevant Au peaks (4p, 4d, and 4f) appeared at 546, 335, and 84 eV, respectively, in the spectrum. The presence of these peaks is consistent with the low grafting density or the small film thickness of the polymer brush. The escape depth of the core electrons (5–10 nm) is larger than the film thickness, so it is possible that the existence of the Au

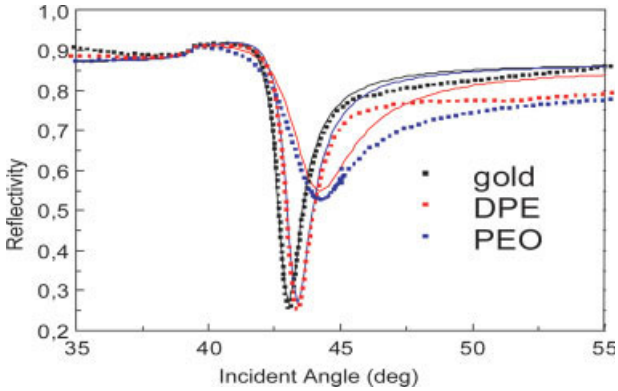

Figure 5. SPS spectrum of the PEO homopolymer brush.

peaks is due to the small film thickness. To confirm this statement, the wetting properties of the PEO brush were studied. The advancing water contact angle was 45° ± 2°, which is close to values reported in the literature (35–45°). This value indicates that the PEO brush has high surface coverage because the nature of the modified (SAM-DPE) Au surface changed dramatically from 110° to 45° after the formation of the brush.

The AFM images indicated a uniform PEO film (RMS 0.4–0.6), with high surface coverage [Fig. 4(b)]. The reason for the very high grafting density could be the low T_g of the PEO, which allows the polymer chains to have enough mobility at room temperature to occupy a large surface area with respect to the surface energy. After annealing at 100 °C overnight in a vacuum oven, the grafting density seemed to be even higher and the morphology consisted of larger, more uniform spherical domains.

Tethered Block Copolymer Brushes on Au Surfaces

Block copolymer brushes of PS-*b*-PEO and PI-*b*-PMMA were synthesized following the same experimental procedure for the homopolymers. The polymerizations were carried out in custom-made glass reactors (Fig. 1), using high vacuum techniques. In both cases the polymerization of the first monomer, styrene or isoprene, was allowed to proceed for 4 h at −78 °C, followed by the addition of the second monomer. The first monomer was added in large amounts, ~10 g, to form a concentrated monomer solution (~25%) to promote the diffusion of the monomer to the living anions on the surface. The amount of the first monomer remaining, after the introduction of the second into the reactor, cannot affect the block copolymerization. In both cases, it is not possible to form tapered or alternating copolymer brushes. The detailed schematic diagrams for the synthesis of the two brushes are provided in Schemes 2 and 3. As shown in Table 1, both block copolymer brushes formed ultrathin films, not expected when using THF as solvent. In our previous paper,[21] we reported the synthesis of homopolymers and block copolymers brushes in benzene. The thickness of the tethered polymers was between 5 and 25 nm. We had seen that by addition of small amounts of polar additives such as tetramethylethylenediamine (TMEDA) and THF in the nonpolar solvent (benzene), the thickness of the polymer brushes on Au substrates increased. On the basis of these results, we believed that the presence of a polar additive facilitated the polymerization at the interface, where the propagating anions created a more polar interface and the access of the monomers could be enhanced.[21] Since the monomers (St, I, Bd) and the solvent (benzene) were nonpolar, in all polymerization there was a large difference in surface tension between the polar interface of the living anions and the nonpolar environment of the solution, which can prevent the diffusion of monomers to the living initiation sites on the surface. This would result in the formation of polymer brushes with low thickness with respect to the slow propagation rate of the monomers. However, using more polar monomers (MMA, EO) and solvent (THF) no significant change in the brush thickness was observed. It seems that the low concentration of the living anions on the surface plays a crucial role.

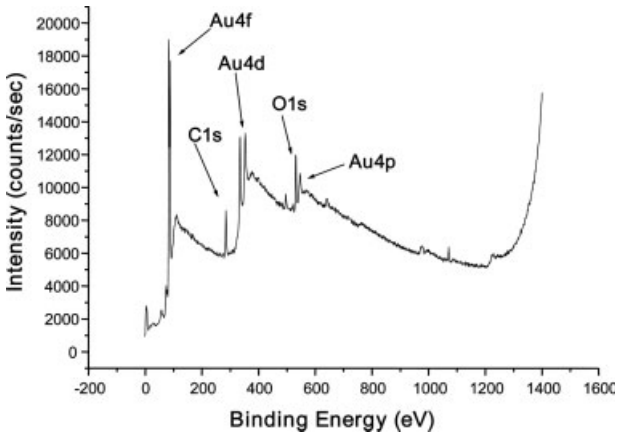

Figure 6. XPS spectrum of the PEO homopolymer brush.

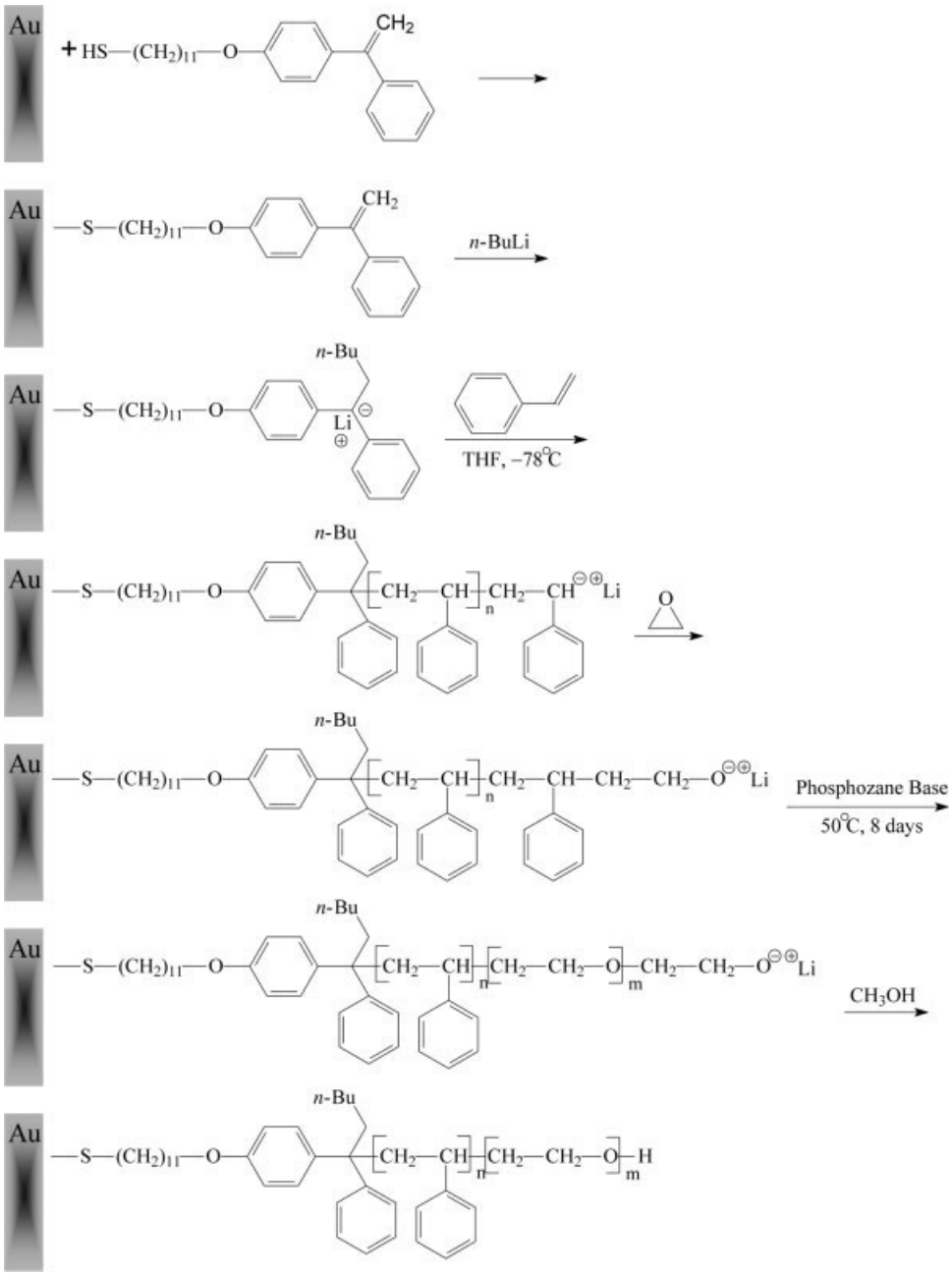

Scheme 2. The schematic diagram for the formation of PS-*b*-PEO block copolymer brush on an Au surface.

The thickness of the PS-*b*-PEO, as measured by SPS, was 7 nm (Fig. 7). The presence of the two blocks in the polymer brush was confirmed by FTIR analysis (Fig. 8). The peak at 1500–1600 cm^{-1} corresponds to C—C aromatic stretching vibrations, those between 2850 and 2990 cm^{-1} to aliphatic CH stretching vibrations (Al—CH), and the peak at 100–1200 cm^{-1} to C—O—C vibrations. The spectrum was background-subtracted from the glass adsorption (due to a thinner reflecting Au surface, only 45 nm). The wetting properties of this brush were also studied. We had previously measured the advancing water contact angles for both PS and PEO homopolymers on gold substrates. The advancing water contact angle for the PS-*b*-PEO block copolymer was measured at $63^\circ \pm 2^\circ$. This value was between the two reported values (94°, 45°) for the two homopolymer brushes.

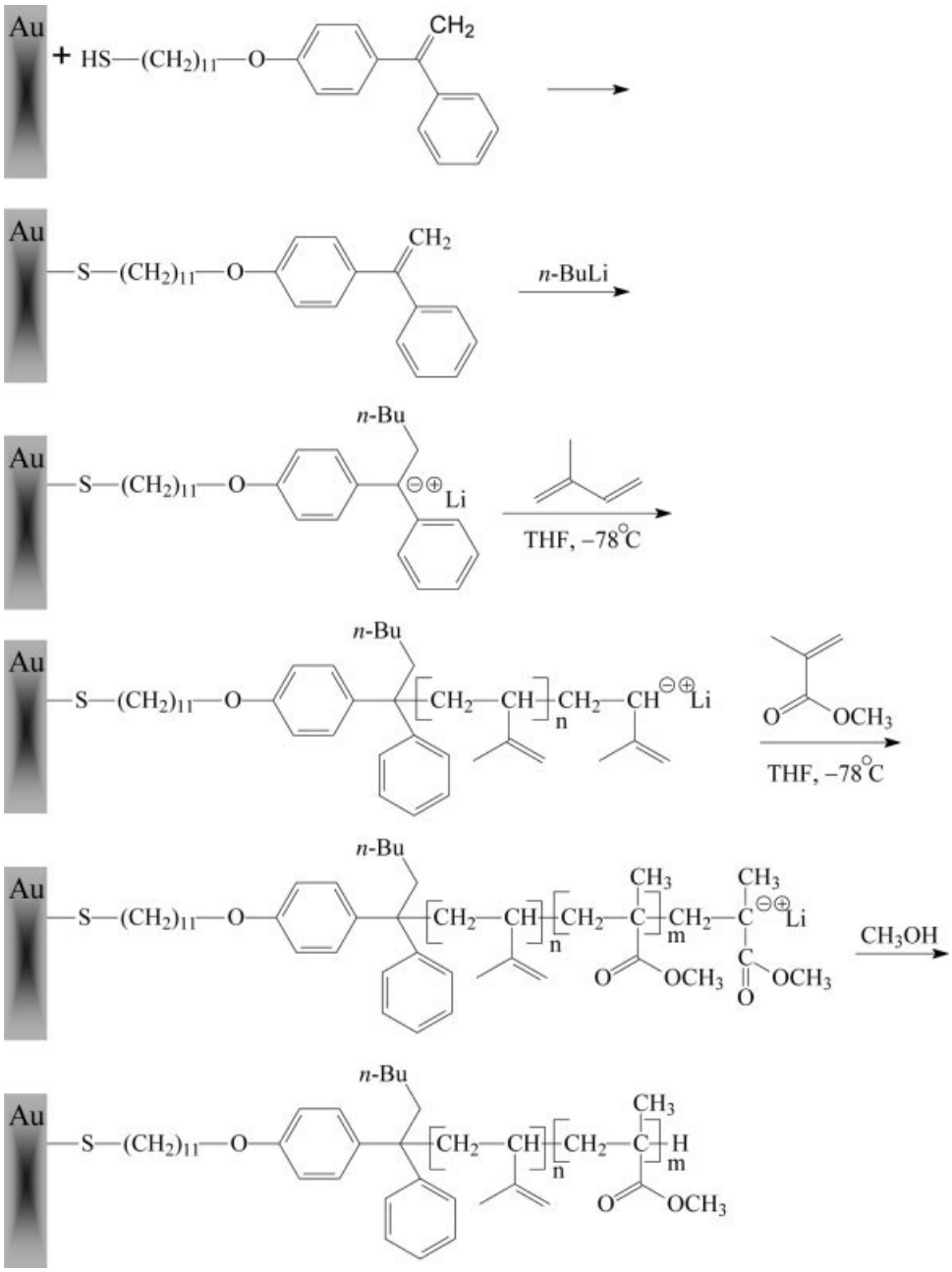

Scheme 3. The schematic diagram for the formation of PI-*b*-PMMA block copolymer brush on an Au surface.

We would expect that the value of the advancing water contact angle of the tethered diblock brush should be around 45°, since it has been reported[23] that even one monomeric unit of ethylene oxide at the end of a grafted PI brush changed the advancing water contact angle from 86° to 47°. We assume that the reason for the high value of the contact angle is the large interaction parameter, χ, between the two blocks, along with the higher surface energy, γ, of PEO block compared with that of the PS block. A high value of χ, would result in the minimization of the interfacial area between the two blocks. The PEO chains would aggregate to avoid contact with the PS chains and because $\gamma_{PEO} > \gamma_{PS}$ the brushes would tend to reorganize to maximize the amount of PEO at the surface and to minimize the surface contacts of PS chains. Hence, it would be easier for the tethered PS chains to increase their contact area with the air interface. A phase separation of the two blocks after this

Table 1. Preparation Conditions, Thickness, and Contact Angles of Homopolymers and Copolymers Grown by Anionic SIP

Sample	Initiator	Solvent	Thickness (nm)	Contact Angle (deg)
PEO	*n*-BuLi	THF	6.0	45
PS	*n*-BuLi	THF	14.0	94
PS-*b*-PEO	*n*-BuLi	THF	7.0	63
PI-*b*-PMMA	*n*-BuLi	THF	6.0	73

reorganization of the polymer brushes, at the surface, was expected. However, this was not observed by AFM (Fig. 9) and the most likely reason is the small thickness (low molecular weight of the tethered polymer chains) of the film. Also this film exhibits different surface properties in response to different solvent conditions. It is known[60] that block copolymer brushes tend to reorganize when they are in contact with different environments. The Au substrate was immersed in methylene chloride (a good solvent for both blocks) for 3 h and the advancing water contact angle was estimated at 60° ± 2°. The substrate was subsequently treated with cyclohexane at 35 °C (a theta solvent for PS and nonsolvent for PEO block) for another 3 h and the advancing water contact angle was estimated at 87° ± 2°.

The XPS spectrum for the tethered diblock copolymer brush PI-*b*-PMMA is shown in Figure 10(a). The peaks at 284.5 and 532 eV correspond to the C 1s and O 1s core electrons, respectively, indicating the presence of the PMMA block. However, Au relevant peaks were again present at 335 eV 4d and at 84 eV 4f. The ratio of these peaks was comparable with that of the peaks corresponding to C 1s and O 1s. As reported earlier, this is consistent with the small thickness of the film, which was measured as 6.0 nm by SPS, or low grafting density. However, there was no evidence of low grafting density by the AFM images (Fig. 11). It is also important to note that the Au peaks have a much higher sensitivity factor for photoelectron transitions compared with C (C/Au of 1:17), and this may explain why Au peak intensities are higher compared with the actual constitution. From the analysis of the spectrum [Fig. 10(a)] there is no evidence for the presence of the PI block. To confirm the existence of the PI, bromination experiments were performed on the polymer brush.[61] The carbon–carbon double bonds should be reactive to bromination if a PI block is present. Hence, bromination took place in a sealed chamber for a few minutes by evaporating Br_2 directly in the path of the substrate. The relevant peaks, Br 3s 255 eV, Br $3p_{1/2}$ 188 eV, Br $3p_{3/2}$ 182 eV, Br 3d 69 eV, verify the presence of the PI block. In addition, water contact angle measurements were carried out. The PI homopolymer brush is reported to have an advancing water contact angle of ~86° ± 2°. The advancing water contact angle of the PI-*b*-PMMA brush was measured as 73° ± 2°, in good agreement with values reported in the litera-

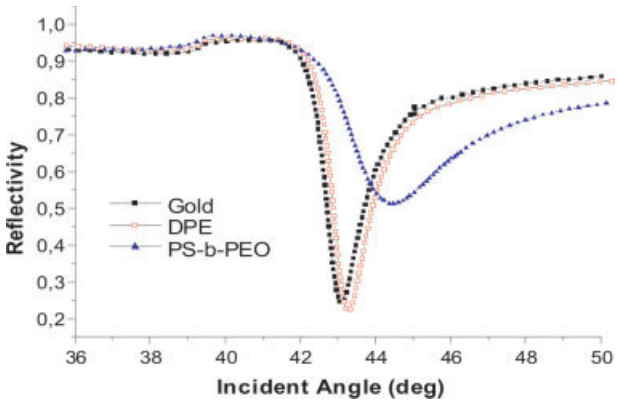

Figure 7. SPS spectrum of the PS-*b*-PEO block copolymer brush.

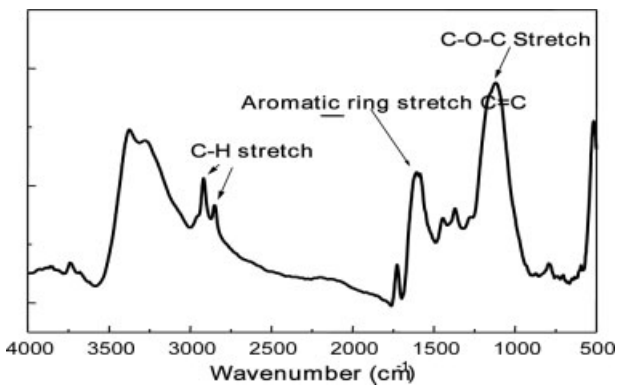

Figure 8. FTIR spectrum of the PS-*b*-PEO block copolymer brush.

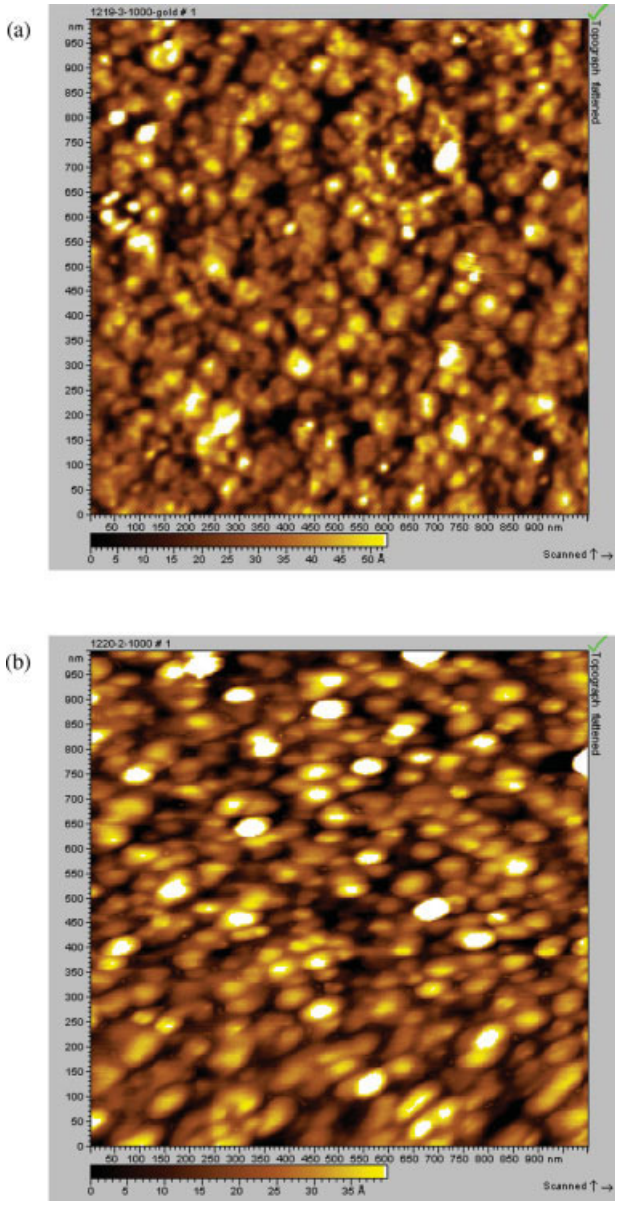

Figure 9. (a) AFM images of PS-*b*-PEO diblock copolymer brush. The topological or height image before annealing. (b) AFM images of PS-*b*-PEO diblock copolymer brush. The topological or height image after annealing at 120 °C.

ture. High-resolution XPS experiments are in progress to estimate the polymer composition with respect to the bromination.

CONCLUSIONS

Homopolymer and diblock copolymer brushes were synthesized by living anionic surface-initiated polymerization on gold substrates. SAM-DPE activated by *n*-BuLi was utilized as the initiator mechanism. Surface-sensitive analytical techniques, including ellipsometry, SPS, AFM, QCM, XPS and FTIR, were used to confirm the presence of the SAMs and of the polymer brushes. The wetting properties as well as the response of the tethered diblock copolymers at different solvent environments were studied by water contact angle measurements. Low surface initiator concentrations and experimental conditions seem to be the crucial parameters for the small film thickness. The use of polar media and absence of impurities are critical in facilitating grafting via surface-initiated anionic polymerization methods. Future investigations will target the synthesis of thick diblock copolymer brushes, with controlled compositions, to clarify the influence of a number of parameters, including the immobilization of the one end of the polymer chain on the substrate, the Flory interaction parameter, χ, the grafting density, the total M_w, the volume fraction and the surface energy, γ, of each block on the tendency for microphase separation.

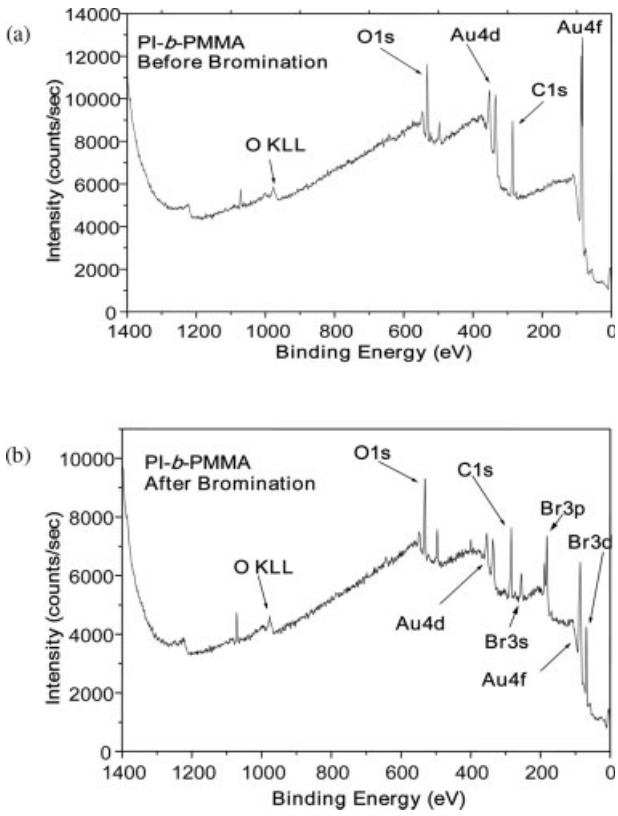

Figure 10. XPS spectra of the PI-*b*-PMMA grafted diblock copolymer brush (a) before and (b) after bromination.

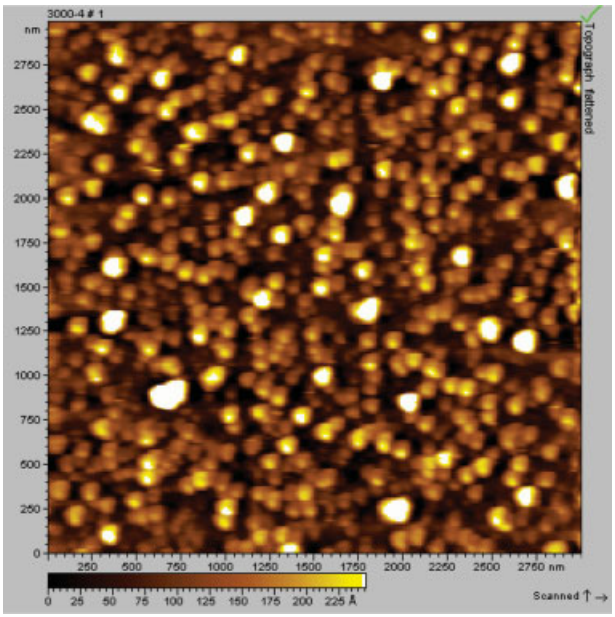

Figure 11. AFM images of PI-*b*-PMMA diblock copolymer brush. The topological or height image.

The Research Committee of the University of Athens and the financial support of the Ministry of Education through the PYTHAGORAS postdoctoral program: "Support of the research groups in the Universities," cofinanced from the Operational Programme and Initial Educational Vocational Training–EPEAEK and the European Social Funds, are greatly appreciated. In addition, we thank the U.S. National Science Foundation for support through its Collaborative Research in Chemistry Program (CRC-CHEM 0304807) and DMR-0315565.

REFERENCES AND NOTES

1. Polymer Brushes; Advincula, R.; Ruehe, J.; Brittain, W.; Caster, K. Eds. VCH-Wiley: Weinheim, 2004, 483 p.
2. (a) Halperin, A.; Tirrell, M.; Lodge, T. P.; Adv Polym Sci 1992, 100, 31; (b) Milner, S. T. Science 1991, 251, 905.
3. Szleifer, I.; Carignano, M. A. Adv Chem Phys 1996, 94, 165.
4. Park, M.; Harrison, C.; Chaikin, P. M.; Register, R. A.; Adamson, D. H. Science 1997, 276, 1401.
5. Martin, C. H. Science 1994, 266, 1961.
6. Huang, E.; Russell, T. P.; Harrison, C.; Chaikin, P. M.; Register, R. A.; Hawker, C. J.; Mays, J. Macromolecules 1998, 31, 7641.
7. Zhao, B.; Brittain, W. J. Prog Polym Sci 2000, 25, 677.
8. Klein, J.; Kamiyama, Y.; Yoshizawa, H.; Israelachvili, J. N.; Frederickson, G. H.; Pincus, P.; Fetters, L. J. Macromolecules 1993, 26, 5552.
9. Fytas, G.; Anastasiadis, S. H.; Seghrouchni, R.; Vlassopoulos, D.; Li, J.; Factor, B. J.; Theobald, W.; Toprakcioglu, C. Science 1996, 274, 2041.
10. Luzinov, I.; Julthongpiput, D.; Tsukruk, V. V. Macromolecules 2000, 33, 7629.
11. Ejaz, M.; Yamamoto, S.; Ohno, K.; Tsujii, Y.; Fukuda, T. Macromolecules 1998, 31, 5934.
12. Ingall, M. D. K.; Honeyman, C. H.; Mercure, J. V.; Bianconi, P. A.; Kunz, R. R. J Am Chem Soc 1999, 121, 3607.
13. Husseman, M.; Malmstrom, E. E.; McNamara, M.; Mate, M.; Mecerreyes, D.; Benoit, D. G.; Hedrick, J. L.; Mansky, P.; Huang, E.; Russell, T. P.; Hawker, C. J. Macromolecules 1999, 32, 1424.
14. Matyjaszewski, K.; Miller, P.; Shukla, N.; Immaraporn, B.; Gelman, A.; Luokala, B. B.; Siclovan, T. M.; Kickelbick, G.; Vallant, T.; Hoffman, H.; Pakula, T. Macromolecules 1999, 32, 8716.
15. Husemann, M.; Mecerreyes, D.; Hawker, C. J.; Hedrick, J. L.; Shah, R.; Abbott, N. L. Angew Chem Int Ed 1999, 38, 647.
16. Kim, N. Y.; Jeon, N. L.; Choi, I. S.; Takami, S.; Harada, Y.; Finnie, K. R.; Girolami, G. S.; Nuzzo, R. G.; Whitesides, G. M.; Laibinis, P. E. Macromolecules 2000, 33, 2793.
17. Zhao, B.; Brittain, W. J. Macromolecules 2000, 33, 342.
18. Kim, J.-B.; Bruening, M. L.; Baker, G. L. J Am Chem Soc 2000, 122, 7616.
19. Boyes, S. G.; Brittain, W. J.; Weng, X.; Cheng, S. Z. D. Macromolecules 2002, 35, 4960.
20. Wu, T.; Efimenko, K.; Genzer, J. J Am Chem Soc 2002, 124, 9394.
21. Advincula, R.; Zhou, Q.; Park, M.; Wang, S.; Mays, J.; Sakellariou, G.; Pispas, S.; Hadjichristidis, N. Langmuir 2002, 18, 8672.
22. Baum, M.; Brittain, W. J. Macromolecules 2002, 35, 610.
23. Quirk, R. P.; Mathers, R. T.; Cregger, T.; Foster, M. D. Macromolecules 2002, 35, 9964.
24. Schmidt, R.; Zhao, T. F.; Green, J. B.; Dyer, D. J. Langmuir 2002, 18, 1281.
25. Jones, D. M.; Brown, A. A.; Huck, W. T. S. Langmuir 2002, 18, 1265.
26. Xu, F. J.; Zhong, S. P.; Yung, L. Y. L.; Kang, E. T.; Neoh, K. G. Biomacromolecules 2004, 5, 2392.
27. Zhao, B.; He, T. Macromolecules 2003, 36, 8599.
28. Yu, W. H.; Kang, E. T.; Neoh, K. G. Langmuir 2004, 20, 8294.
29. Huang, X. Y.; Wirth, M. J Anal Chem 1997, 69, 4577.
30. (a) Prucker, O.; Ruhe, J. Macromolecules 1998, 31, 592; (b) Prucker, O.; Ruhe, J. Macromolecules 1998, 31, 602.
31. Sheth, S. R.; Leckband, D. Proc Natl Acad Sci 1997, 94, 8399.
32. von Werne, T.; Patten, T. E. J Am Chem Soc 1999, 121, 7409.

33. Jordan, R.; West, N.; Ulman, A.; Chou, Y.-M.; Nuyken, O. Macromolecules 2001, 34, 1606.
34. von Werne, T.; Patten, T. E. J Am Chem Soc 2001, 123, 7497.
35. Pyun, J.; Matyjaszewski, K.; Kowalewski, T.; Savin, D.; Patterson, G.; Kickelbick, G.; Huesing, N. J Am Chem Soc 2001, 123, 9445.
36. Perruchot, C.; Khan, M. A.; Kamitsi, A.; Armes, S. P. Langmuir 2001, 17, 4479.
37. Zhou, Q.; Wang, S.; Fan, X.; Advincula, R.; Mays, J. Langmuir 2002, 18, 3324.
38. Blomberg, S.; Ostberg, S.; Harth, E. E.; Bosman, A. W.; van Horn, B.; Hawker, C. J. J Polym Sci Part A: Polym Chem 2002, 40, 1309.
39. Pyun, J.; Jia, S.; Kowalewski, T.; Patterson, G.; Matyjaszewski, K. Macromolecules 2003, 36, 5094.
40. Chen, X.; Armes, S. P. Adv Mater 2003, 15, 1558.
41. Bartholome, C.; Beyou, E.; Bourgeat-Lami, E.; Chaumont, P.; Zydowicz, N. Macromolecules 2003, 36, 7946.
42. Ohno, K.; Koh, K.; Tsujii, Y.; Fukuda, T. Angew Chem Int Ed 2003, 42, 2751.
43. Parvole, J.; Laruelle, G.; Guimon, C.; Francois, J.; Billon, L. Macromol Rapid Commun 2003, 24, 1074.
44. Laruelle, G.; Parvole, J.; Francois, J.; Billon, L. Polymer 2004, 45, 5013.
45. Joubert, M.; Delaite, C.; Bourgeat-Lami, E.; Dumas, P. Macromol Rapid Commun 2005, 26, 602.
46. Baskaran, D.; Mays, J. W.; Bratcher, M. S. Angew Chem Int Ed 2004, 43, 2138.
47. Qin, S.; Qin, D.; Ford, W. T.; Resasco, D. E.; Herrera, J. E. J Am Chem Soc 2004, 126, 170.
48. Kong, H.; Gao, C.; Yan, D. J Am Chem Soc 2004, 126, 412.
49. Ito, Y.; Ochiai, Y.; Park, Y. S.; Imanishi, Y. J Am Chem Soc 1997, 119, 1619.
50. Ito, Y.; Park, Y. S.; Imanishi, Y. J Am Chem Soc 1997, 119, 2739.
51. Ito, Y.; Nishi, S.; Park, Y. S.; Imanishi, Y. Macromolecules 1997, 30, 5856.
52. Ito, Y.; Park, Y. S.; Imanishi, Y. Macromol Rapid Commun 1997, 18, 221.
53. Ulman, A. An Introduction to Ultrathin Organic Films; Academic Press: New York, 1991.
54. Hadjichristidis, N.; Pitsikalis, M.; Pispas, S.; Iatrou, H.; Chem Rev 2001, 101, 3747.
55. Pitsikalis, M.; Pispas, S.; Mays, J. W.; Hadjichristidis, N. Adv Polym Sci 1998, 135, 1.
56. Hadjichristidis, N.; Iatrou, H.; Pispas, S.; Pitsikalis, M. J Polym Sci Part A: Polym Chem 2000, 38, 3211.
57. Knoll, W. Annu Rev Phys Chem 1998, 49, 569.
58. Prucker, O.; Chrstian, S.; Bock, H.; Ruhe, J.; Frank, C.; Knoll, W. In Organic Thin Films; Frank, C.; Ed.; American Chemical Society: Washington, DC, 1998; p 233.
59. Oostreling, M. L. C. M.; Sein, A.; Shouten, A. J. Polymer 1992, 33, 4394.
60. Zhao, B.; Brittain, W. J. J Am Chem Soc 1999, 121, 3557.
61. Buzdugan, E.; Ghioca, P.; Badea, E.; Serban, E.; Stribeck, N. Eur Polym Mater 1997, 33, 1713.